Dual-Band Divider Has Rejection Band at 5 GHz

Article *in* Microwaves and Rf · October 2016

CITATION
1

READS
260

3 authors:

Ahmed Fawzy Daw
Modern Sciences and Arts University
23 PUBLICATIONS **47** CITATIONS
SEE PROFILE

Mahmoud Abdelrahman Abdalla
Military Technical College
222 PUBLICATIONS **1,376** CITATIONS
SEE PROFILE

Hadia M. El-Hennawy
Ain Shams University,Faculty of Engineering,Cairo,Egypt
158 PUBLICATIONS **791** CITATIONS
SEE PROFILE

microwaves&rf

AHMED F. DAW
Lecturer, Microwave Engineering Researcher, Communication and Electronics Department, Faculty of Engineering, MSA University, Cairo, Egypt; e-mail: afali@msa.eun.eg

MAHMOUD A. ABDALLA
Associate Professor in Electromagnetic Waves Group, Electronic Engineering Department, MTC College, Cairo, Egypt; e-mail: maaabdalla@ieee.org

HADIA M. ELHENNAWY
Professor in Antennas and Propagation, Electronics and Communication Department, Ain Shams University, Cairo, Egypt; e-mail: helhennawy@ieee.org

Dual-Band Divider Has Rejection Band at 5 GHz

This compact power divider passes signals from 1.0 to 4.8 GHz and from 6.2 to 9.0 GHz, in addition to including a rejection band to stop WLAN interference from 5.0 to 5.8 GHz.

This compact dual-band ultrawideband (UWB) power divider is designed for multiband orthogonal frequency division multiplexing (OFDM) from 1.0 to 4.8 GHz and for direct sequence ultrawideband applications from 6.2 to 9.0 GHz. It also provides a sharp rejection band from 5.0 to 5.8 GHz to help suppress interference between wireless local-area networks (WLANs) and UWB communications systems.

The power divider, which is based on two unit cells formed of dual composite right/left-handed microstrip transmission lines, exhibits low insertion loss in both passbands. The circuit measures just 16.6 × 20.0 mm^2—some 45.37% smaller than conventional single-band, quarter-wavelength ($\lambda_g/4$) power dividers.

Global expansion of wireless services and systems has driven the need for miniature high-frequency components operating in specific multiple frequency bands, using straightforward design approaches and ease of fabrication.[1-3] The use of metamaterials (engineered materials) has made possible the use of new design methods for improved electrical performance in smaller components.[4,5]

One of these structures is the dual composite right-/left-handed metamaterial transmission line (D-CRLH TL).[6] D-CRLH TLs have been implemented recently in a number of different configurations, yielding good results.[7-10] These planar circuits are fairly simple to realize since they do not require viaholes for ground or circuit connections.

D-CRLH TLs exhibit dual propagation passbands: a right-handed (RH) band at lower frequencies and a left-handed (LH) band at higher frequencies. The circuitry also features a nonlinear phase coefficient through the two bands, making the technology suitable for the design and fabrication of a variety of different microwave components.[11-17] One challenge inherent to the use of D-CRLH TLs, however, lies in achieving effective impedance matching over the wide frequency bands provided by the transmission lines.

Since power dividers are so widely used in high-frequency systems with other RF/microwave components—such as power amplifiers, quadrature frequency mixers, modulators, and phased-array antennas—many researchers attempt to improve these components by reducing the size of impedance transformers for them.[18-20] Some attempts at designing dual-band and wideband power dividers have employed metamaterial structures[21-23] in addition to other approaches.[24-28]

The use of D-CRLH TLs in a microstrip configuration can deliver an extremely broadband two-way, dual-band power divider with fairly consistent performance across its full range

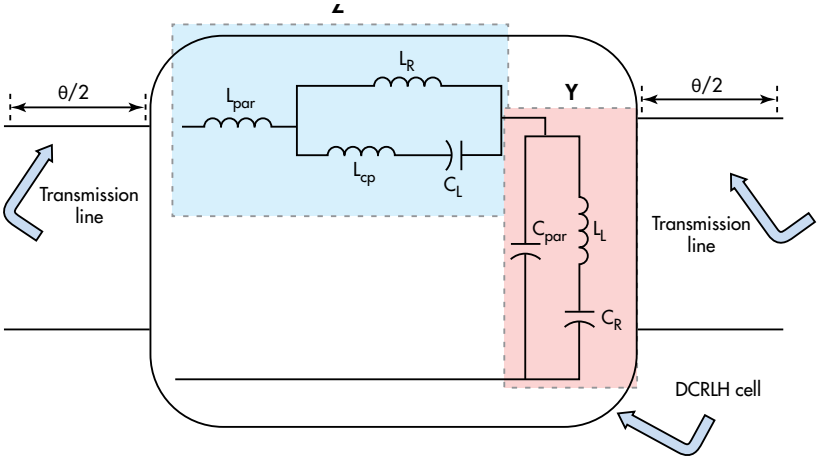

1. This equivalent circuit represents the D-CRLH unit cell.

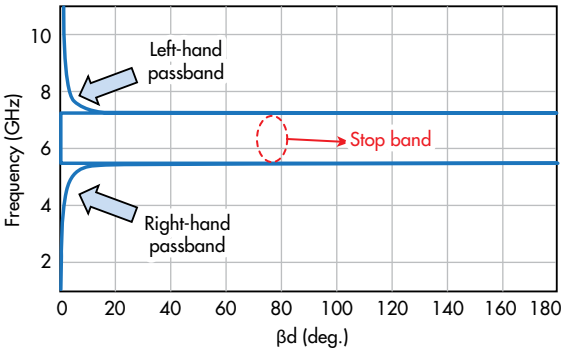

2. This is a dispersion diagram for the 70.7-Ω D-CRLH impedance transformer used in the power divider.

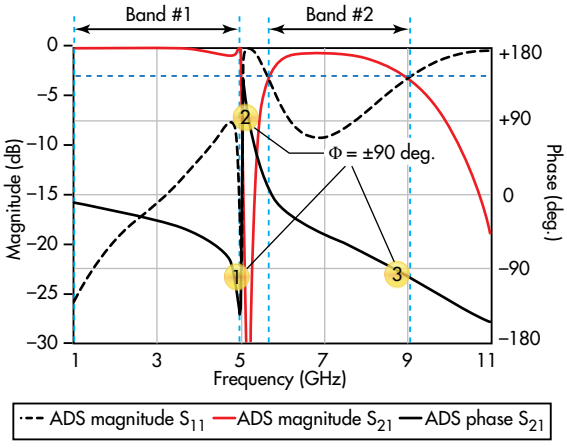

3. The plots show circuit and full-wave simulated transmission-coefficient (S21) magnitude and phase for the 70.7-Ω D-CRLH unit-cell transformer.

of passband frequencies. It offers similar performance across its low-frequency band from 1.0 to 4.8 GHz for MB-OFDM systems and across its high-frequency band from 6.2 to 9.0 GHz for DS-UWB systems.

At the same time, the power divider achieves high isolation in the range of frequencies between the two communications bands, with better than 20-dB rejection of signals in the range from 5.0 to 5.8 GHz, for effective suppression of possible interference from WLAN sources.

Figure 1 shows an equivalent circuit of a D-CRLH TL structure. The circuit consists of a series tank circuit formed with capacitor C_{par} and inductor L_L in series with capacitor C_R. Another tank circuit is formed by capacitor C_L and inductor L_{cp} in series with capacitor C_L. Inductor L_{par} is connected to represent any RH parasitic inductance. The tank circuit is connected to a host transmission line with electrical length θ. The phase along the D-CRLH TL (β_d) can be extracted by applying a periodic analysis of an infinite number of cells, as shown in Eq. 1[5]:

$$\cos(\beta_d) = \cos(\theta) + 0.5[ZY\cos^2(\theta/2)] + i(0.5)(Z_0Z+Y_0Y)\sin(\theta/2) \quad (1)$$

where Z_0 and Y_0 represent the RH characteristic impedances and admittances, respectively; Z is the series branch impedance; and Y is the shunt branch admittance. Modeling the D-CRLH unit cell as a transmission line, its characteristic impedance can be extracted by applying Eq. 2:

$$Z_{CRLH} = (Z/Y)^{0.5} = (j\omega L_{par} + \{[j\omega L_R(1 - \omega^2 L_{cp}C_L)]/ [1 - \omega^2(L_{cp} + L_R)C_L)]\}/\{[j\omega(C_R + C_{par}) - j\omega^3 C_{par}C_R L_L]/(1 - \omega^2 L_L C_R)]\})^{0.5} \quad (2)$$

Design requirements for the impedance transformer include: (1) adjusting the cutoff frequencies to be the lower and upper frequencies of the two desired passbands bands; (2) achieving ±90-deg. progressive phase shifts at the start and end frequencies of the two passbands; and (3) maintaining good impedance matching within the two passbands.

Since the D-CRLH TL circuit is unbalanced, the cutoff frequencies of the middle stopband (4.8 and 6.2 GHz) were designed according to Eq. 1, such that for very small values of θ, the condition $\beta_d = \pi$ is satisfied at the two cutoff frequencies by Eq. 3:

$$-4 = \{[j\omega L_R(1 - \omega^2 L_{par}C_L)]/[1 - \omega^2(L_{par}C + L_R)C_L]\} \times \{[j\omega(C_R + C_{par}) - j\omega^3 C_{par}C_R L_L]/(1 - \omega^2 L_L C_R)]\}\pi_{|f = 4.8\ GHz, 6.2\ GHz} \quad (3)$$

The upper cutoff frequency of the second passband (11 GHz) was achieved by satisfying the condition $\beta_d = 0$ in Eq. 1

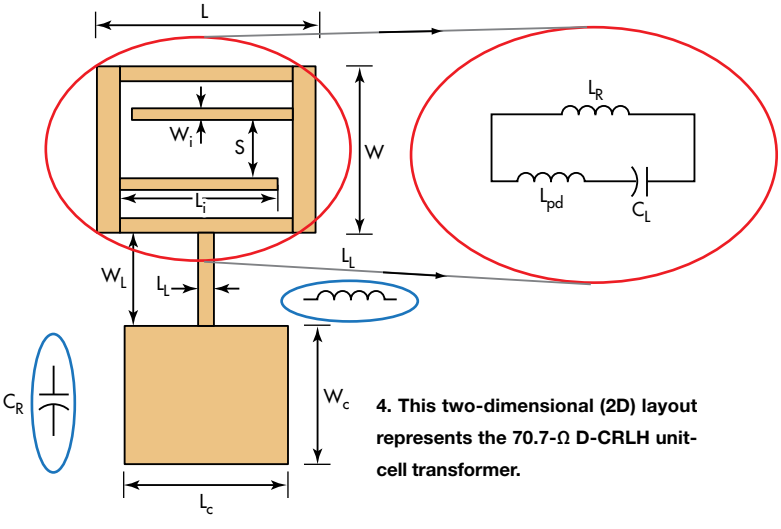

4. This two-dimensional (2D) layout represents the 70.7-Ω D-CRLH unit-cell transformer.

TABLE 1: LOADING ELEMENT VALUES AND DIMENSIONS OF THE D-CRLH UNIT CELL			
Circuit element	Electrical values	Dimensions	Values (mm)
C_L	0.16 pF	L	4.85
L_R	2.11 nH	W	3.416
L_{par}	0.830 nH	W_i	0.2
L_{CP}	3.86 nH	L_i	3.35
C_R	0.23 pF	S	1.3
C_{par}	0.032 pF	L_L	0.3
L_L	0.30 nH	L_C	3
		W_L	2
		W_C	3

for small θ and a minimum (min) frequency of 11 GHz. This can be expressed mathematically by Eq. 4:

$$\min((1/2\pi)\{[1 + (C_{par}/C_R)]/C_{par}L_L\}^{0.5}; \quad (1/2\pi)\{(L_R + L_{par})/C_L[(L_RL_{CP} + L_{par}(L_R + L_{CP})]\}^{0.5}) = 11 \text{ GHz} \quad (4)$$

For effective quarter-wavelength impedance transformations over both passbands, the D-CRLH TL circuitry was designed for −90 deg. at 4.8 GHz (the edge of the RH passband) and +90 deg. at 6.2 GHz (the beginning of the LH passband). These goals can be expressed by Eq. 5:

$$\phi_{DCLRH} = \beta_{d|f = 4.8\ GHz} = -\pi/2,$$

$$\phi_{DCLRH} = \beta_{d|f = 6.2\ GHz} = \pi/2 \quad (5)$$

Impedance matching is adjusted by maintaining the D-CRLH transmission line with

an impedance Z_{DCRLH} of 70.7 Ω near the two passband cutoff frequencies, as shown in Eq. 6:

$$\max(|\Gamma|) = 0.316_{|f = 6.2\ GHz};$$

$$\Gamma = (Z_0 - Z_{DCRLH})/(Z_0 + Z_{DCRLH}) \quad (6)$$

Equations 3-6 were solved numerically using MATLAB simulation software from MathWorks (www.mathworks.com), with results presented in *Table 1*. The cutoff frequencies were validated by plotting the dispersion diagram for the calculated values using Eq. 1, as shown in *Fig. 2*. As can be seen from Fig. 2, the D-CRLH cell achieves a RH passband from dc to 5.7 GHz, and a sharp stopband from 5.7 to 7 GHz, followed by a LH passband from to 7 GHz to beyond 11 GHz.

These cutoff frequencies fulfill the design specifications for the power divider's first passband band (dc to 4.8 GHz), while the performance of the second passband is shifted by approximately 1.5 GHz. This can be considered a limitation of the numerical solution, which will be optimized during the cell realization phase of the design process.

Circuit simulations on the transmission lines and power-divider circuitry were performed with the Advanced Design System (ADS) software from Keysight Technologies (www.keysight.com); simulated transmission and reflection coefficients are plotted in *Fig. 3*. The cell was terminated in 70.7 Ω at both ends during the simulation.

The simulations reveal the two passbands defined according to 3-dB $|S_{21}|$ cutoff points from 1 to 5 GHz and from 5.8 to 9.1 GHz. Within the first passband,

$|S_{21}|$ is extremely minimal, from 0 to −0.2 dB, with very low reflection coefficient

$|S_{11}|$ of −10 to −26 dB.

The second passband has lower $|S_{21}|$ values, −1 dB at the lower frequencies and dropping to −3 dB at the higher frequencies. The ±90-deg. phase conditions are validated by plotting the magnitude and phase of $|S_{21}|$ as shown in Fig. 3. As can be seen, the progressive phase is ±90 deg. within the passband at 4.85, 5.4, and 8.85 GHz. The second phase at 5.4 GHz is a bit shifted due to oversimplification of the circuit model.

The simulations indicate that the power divider will function with acceptable performance within the two OFDM/DS-UWB bands (1.0 to 4.8 GHz and 6.2 to 9.2 GHz). To evaluate actual circuitry, the D-CRLH power divider was fabricated with the layout of *Fig. 4*. The D-CRLH cell consists of an interdigital capacitor shunted with a strip inductor, followed by a series inductor with a patch capacitor.

The cell is based on low-loss printed-circuit-board (PCB) material from Rogers Corp. (www.rogers.com) with relative dielectric constant (ε_r) of 3.55 and thickness of 1.52 mm. The

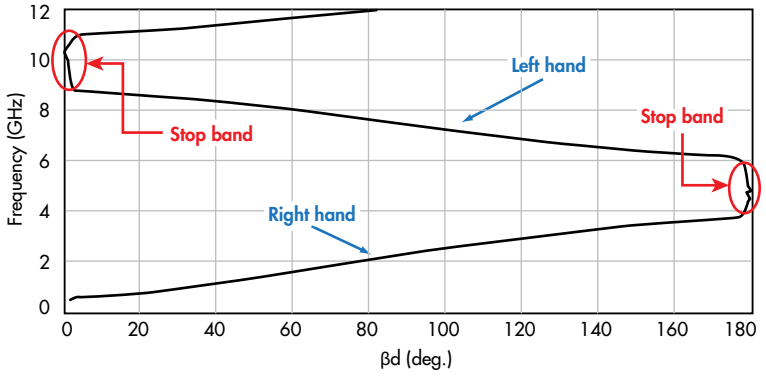

5. This is a dispersion diagram of the 70.7-Ω D-CRLH D-CRLH TL used in the dual-band power divider.

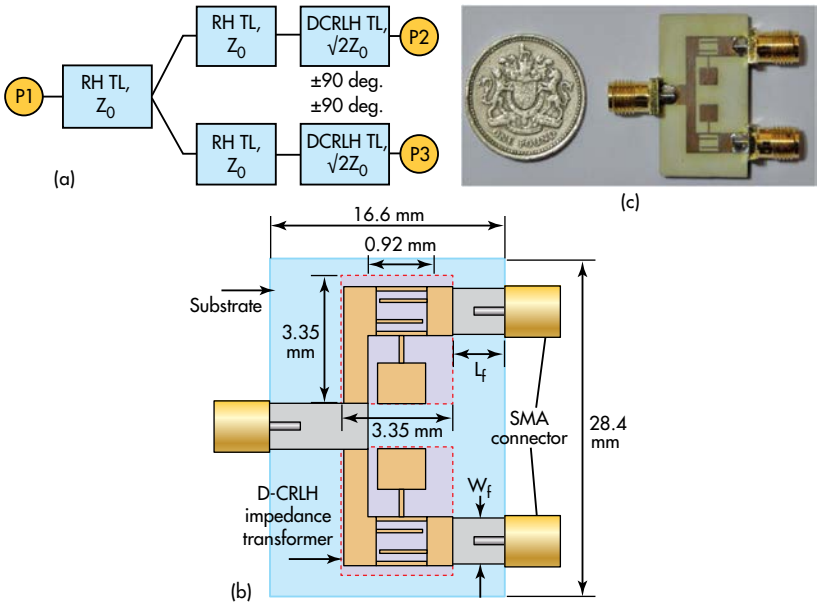

6. The design process for the D-CRLH power divider included (a) the block diagram, (b) a 2D layout with Lf = 5 mm and Wf = 3.45 mm, and the prototype fabricated on commercial PCB material.

dimensions of the circuitry were extracted according to Eq. 7[29]:

$$L = (Z_c/\omega)\tan(\beta l_L),$$

$$C_I\,(\text{pF}) = 3.937 \times 10^{-5}\, l_I(\varepsilon_r + 1)[0.11(n - 3) + 0.252] \quad (7)$$

where L is the inductance of the stripline; l_L is the length of the strip inductor; z_c is the characteristic impedance of the strip inductor; C_I is the interdigital capacitance; l_I is the width of the interdigital capacitor; and n is the number of interdigital capacitor fingers. The capacitor finger length was chosen for a given finger spacing that could be practically fabricated.

Based on the calculated dimensions of the strip inductor, some fine-tuning was performed. CST Microwave Studio (www.cst.com) three-dimensional (3D) electromagnetic (EM) simulation software was used to achieve the final circuit element dimensions listed in Table 1.

To confirm the behavior of the D-CRLH cell, simulated full-wave S-parameters were used to create the dispersion diagram of *Fig. 5*. It starts with RH behavior within the first passband extending from dc to 4 GHz. The stopband extends from 4.3 to 5.8 GHz. The second passband, with LH behavior, extends from 6.2 to 11 GHz.

Figure 6(a) shows a block diagram of the two-way power divider. It employs one cell of the dual-band impedance transformer in each branch of the divider. *Figure 6(b)* shows a layout for the dual-band D-CRLH power divider, which is designed to equally divide power applied between its input port and the two output ports. The miniature power divider measures just 21.4×16.6 mm^2 or $0.27 \times 0.22\lambda_g^2$, where wavelength λ_g is calculated at the midband frequency of the first passband. *Figure 6(c)* shows the prototype power divider fabricated on commercial PCB material.

S-parameter magnitudes of the D-CRLH power divider were measured with a commercial, two-port vector network analyzer (VNA). *Figure 7(a)* provides a comparison between measured and full-wave simulated S_{21} results for the D-CRLH

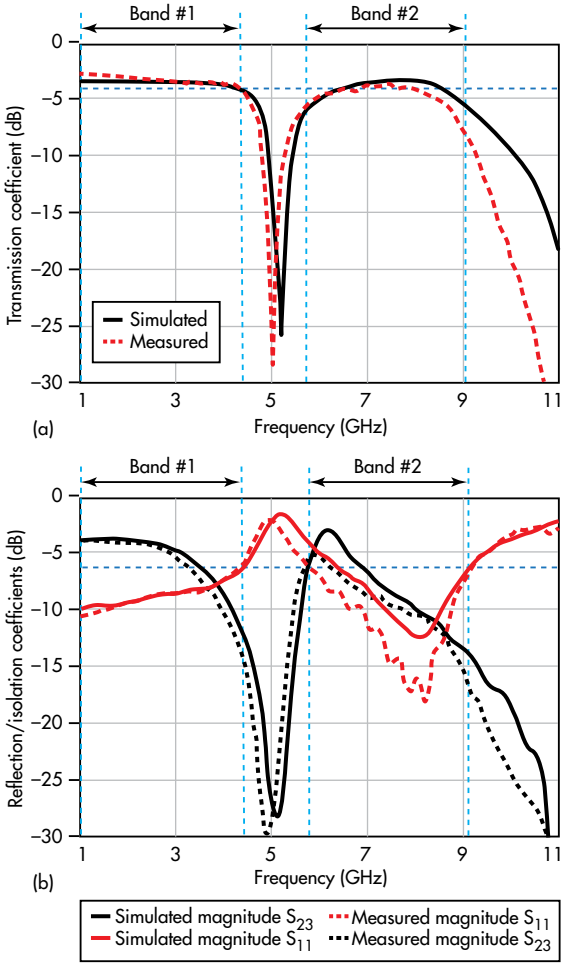

7. The plots show full-wave simulated and measured results for the two-way power divider: (a) transmission coefficient (S21) and (b) reflection (S11) and isolation (S23) coefficients.

TABLE 2: COMPARING THE EXPERIMENTAL POWER DIVIDERS WITH PREVIOUS WORK						
Source	Bands	Size (mm^2)	Size (λ_g^2)	Frequency (GHz)	Insertion loss (dB)	Return loss (dB)
This work	2	16.6 × 20.4	0.22 × 0.27 0.72 × 0.88	1.0 to 4.7 6.2 to 9.0	3.3 ± 0.3	10
Ref. 23	2	22.5 × 25	0.19 × 0.22 0.67 × 0.76	1.0 to 2.78 6.25 to 7.1	3.0 ± 0.5	10
Ref. 24	1	12.9 × 43.48	0.4 × 1.37	3.1 to 10.6	3.0 ± 0.5	11
Ref. 25	1	22 × 16.33	0.29 × 0.22	1.8 to 2.45	3.0 ± 0.5	30
Ref. 26	2	24 × 24	0.27 × 0.35 0.39 × 0.5	3.5 to 5.0	3.0 ± 0.9	13-15

power divider, with reflection coefficient (S_{11}) and isolation coefficient (S_{23}) results in *Fig. 7(b)*.

These results show the two passbands from 1 to 4.8 GHz and 6.2 to 9 GHz with good agreement between measurements and simulations. The S_{21} magnitude is better than −4 dB throughout the two passbands. Better performance is achieved in the first passband, where S_{21} is about 3.3 dB across the full band.

In the upper passband, the measured S_{21} drops from −4 dB at 8.4 GHz to −6 dB at 9 GHz. For S_{11}, the simulated and measured values are both below −6 dB for both passbands. Isolation differs for the two bands, with performance of about −4 dB for the lower passband and better than −6 dB for the higher passband.

Considering that the power divider is a modified T-junction, with best-case loss of about −6 dB, it provides reasonable isolation. The stopband, for rejection of WLAN signals, extends from 4.8 to 5.8 GHz, with S_{21} reaching −33 dB at 5 GHz. Within this stopband, the return loss reaches 2 dB at 5 GHz.

The design tradeoffs for this power divider include good return and insertion losses for the two passbands and high attenuation within the stopband, at the same time maintaining good isolation between the two output ports. These electrical characteristics were pursued while also attempting mechanical miniaturization of the power divider. The design offers competitive results with some of the latest power-divider designs *(Table 2)*, while being about 45.37% smaller than a conventional design.

REFERENCES

1. P. Sarkar, R. Ghatak, M. Pal, and D.R. Poddar, "High-Selective Compact UWB Bandpass Filter with Dual Notch Bands," IEEE Microwave and Wireless Components Letters, Vol. 21, No. 11, July 2014, pp. 448-450.
2. X.B. Wei, G.T. Liao, J.X. Wang, Z.Q. Xu, and Y. Shi, "Compact Dual-band Bandpass Filter with Ultra-wide Upper-stopband," IET Electronics Letters, Vol. 49, No. 11, 2013, pp 708-709.
3. M. Abedian, S.K.A. Rahim, S. Danesh, S. Hakimi, L.Y. Cheong, and M.H. Jamaluddin, "Novel Design of Compact UWB Dielectric Resonator Antenna with Dual Band Rejection Characteristic for WiMAX/WLAN Bands," IEEE Antennas and Wireless Propagation Letters, Vol. 14, 2015, pp. 245-248.
4. C. Caloz and T. Itoh, Electromagnetic Metamaterials Transmission Line Theory and Microwave Applications, Wiley, New York, 2006.
5. G.V. Eleftheriades and K.G .Balmain, Negative Refractive Metamaterials, Wiley, New York, 2005.
6. Christophe Caloz, "Dual Composite Right/Left-Handed (D-CRLH) Transmission Line Metamaterial," IEEE Microwave and Wireless Components Letters, Vol. 16, No. 11, 2006, pp. 585-587.
7. B. Li, J.P. Yong, and W. Wu, "A Planar Microstrip Implementation of Dual Composite Right/Left Handed Transmisiion Line," 2008 IEEE International Conference on Microwave and Millimeter Wave Technology (ICMMT), Vol. 4, Nanjing, China, 2008, pp 1,617-1,619.
8. A. Belenguer, J. Cascon, A.L. Borja, H. Esteban, and V.E. Boria, "Dual Composite Right-/Left-Handed Coplanar Waveguide Transmission Line Using Inductively Connected Split-Ring Resonators," IEEE Transactions on Microwave Theory & Techniques, Vol. 60, No. 10, 2012, pp. 3,035-3,042, 2012.
9. Young-Ho Ryu, Jae-Hyun Park, Jeong-Hae Lee, Joon-Yub Kim, and Tae Heung-Sik, "DGS Dual Composite Right/Left Handed Transmission Line," IEEE Microwave and Wireless Components Letters, Vol. 18, No. 7, 2008, pp. 434-436.
10. Daniel Decle Colin and Zhirun Hu, "Uniplanar metamaterial based dual composite right-/-left handed (D-CRLH) microstrip line for microwave circuit applications," Proceedings of the 2014 Asia-Pacific Microwave Conference (APMC), 2014, pp. 211-213.
11. Ahmed F. Daw, Mahmoud A. Abdalla, and Hadya M. Elhennawy, "Dual Band High Selective Compact Transmission Line Gap Resonator," 2014 Loughborough Antennas & Propagation Conference, United Kingdom, 2014, pp. 91-94.
12. Ahmed F. Daw, Mahmoud A. Abdalla, and Hadia M. EL-Hennawy, "Multiband Sharp-Skirt Compact Gap Resonator Based D-CRLH," 2015 32th National Radio Science Conference (NRSC), Egypt, pp. 43-50.
13. I.A. Mocanu and T. Petrescu, "Novel dual band hybrid rat-race coupler with CRLH and D-CRLH transmission lines," 2011 Proceedings of the 2011 Asia-Pacific Microwave Conference (APMC), 2011, pp. 888-891.
14. V. González-Posadas, J.L. Jiménez-Martín, A. Parra-Cerrada, L.E. Garcııa-Munıoz, and D. Segovia-Vargas, "Dual-composite right-left-handed transmission lines for the design of compact diplexers," IET Microwaves, Antennas & Propagation, Vol. 4, No. 8, 2010, pp. 982-990.
15. D. Kholodnyak, V. Turgaliev, and E. Zameshaeva, "Dual-band Immittance Inverters on Dual-composite Right/Left-handed Transmission Line (D-CRLH)," GeMIC 2015, Nuremberg, Germany, 2015, pp. 60-63.
16. M.A. Abdalla and A. Fouad, "Ultra Compact Triple Band D-CRLH Metamaterial Antenna," 2015 IEEE International Symposium on Antennas and Propagation & USNC/URSI National Radio Meeting, Vancouver, Canada, 2015, pp. 1,190-1,191.
17. H.N. Quang and H. Shirai, "A Compact Tri-Band Metamaterial Antenna for WLAN and WiMAX Applications," 2015 International Conference on Electromagnetic in Advanced Application (ICEAA), Torino, Italy, 2015, pp. 131-136.
18. M.A. Abdalla and Z. Hu, "Compact tunable left handed ferrite transformer," Journal of Infrared, Millimeter, and Terahertz Waves, Vol. 30, No. 8, 2009, pp. 813-825.
19. M.A. Abdalla and Z. Hu, "Multi-band functional tunable LH impedance transformer," Journal of Electromagnetic Wave and Applications, Vol. 23, 2009, pp. 39-47.
20. Ahmed F. Daw, Mahmoud A. Abdalla, and Hadia M. Elhennawy, "New Inductor Loaded Composite Right Left hand Impedance Transformer for UWB Wireless Applications," Proceedings of the 9th International Congress on Advanced Electromagnetic Material in Microwave and Optics, United Kingdom, September 7-12, 2015, pp. 231-233.
21. Mahmoud A. Abdalla, and Z. Hu, "Compact and Broadband Left handed CPW Power Divider/Combiner for C/X bands," 29th National Radio Science Conference (NRSC 2012), Cairo, Egypt, April 10-12, 2012, pp. 29-36.
22. Mahmoud A. Abdalla and Z. Hu, "Compact Novel CPW Ferrite Coupled Line Circulator with Left-handed Power Divider/Combiner," 2011 European Microwave Week Digest, United Kingdom, 2011, pp. 794-797.
23. Guo-cheng Wu, Guangming Wang, Jia-jia Sun, Xiang-jun Gao, and Ya-wei

Wang, “Compact dual-band power divider based on dual composite right/left-handed transmission line,” Electronics Letters, vol. 50, No. 10, May 2014, pp. 759-761.
24. Wei-Qiang Liu, Feng Wei, Chun-Hui Pang, and Xiao-Wei Shi, “Design of a Compact Ultra-Wideband Power Divider,” International Conference on Microwave and Millimeter Wave Technology (ICMMT), Shenzhen, China, 2012, pp. 1-3.
25. Da Kang, Yi-Hsin Pang, and Hsin-Hao Chen, “Compact Wilkinson Power Divider/ Combiner with Two-Section Coupled Lines for Harmonics Suppression,” 2012 Asia-Pacific Microwave Conference (APMC), Taiwan, 2012, pp. 995-997.
26. Qun Li, Yonghong Zhang, and Yong Fan, “Dual-band In-phase Filtering Power Dividers Integrated with Stub-loaded Resonators,” IET Microwave and Antennas Propagation, Vol. 9, No. 7, 2015, pp. 695-699.
27. Nanjing Geo, Guoan Wu, and Qinhua Tang, “Design of a Novel Compact Dual-Band Power Divider with Wide Frequency Ratio,” IEEE Microwave and Wireless Components Letters, Vol. 24, No. 2, 2014, pp. 81-83.
28. Geo-Le Dai, Xing-Chang Wei, Er-Ping Li, and Ming-Yao Xia, “Novel Dual Band Out-of-Phase Power Divider with High Power Handling Capability,” IEEE Transactions on Microwave Theory & Techniques, Vol. 60, No. 8, 2012, pp. 2,403-2,409.
29. J.S. Hong and M.J. Lancaster, Microstrip Filter for RF/Microwave Appications, Wiley, New York, 2001.